Proceedings of the 26th Annual International Conference of the IEEE EMBS
San Francisco, CA, USA • September 1-5, 2004

Visualizing Early Frog Development with Motion-Sensitive 3-D Optical Coherence Microscopy

R. C. Haskell[1], M. E. Williams[2], D. C. Petersen[1], B. M. Hoeling[1], A. J. Schile[2], J. D. Pennington[2], M. G. Seetin[1], J. M. Castelaz[1], S. E. Fraser[3], C. Papan[3], H. Ren[4], J. F. de Boer[5], Z. Chen[4]
[1]Department of Physics, Harvey Mudd College, Claremont, CA, USA
[2]Department of Biology, Harvey Mudd College, Claremont, CA, USA
[3]Biological Imaging Center, California Institute of Technology, Pasadena, CA, USA
[4]Beckman Laser Institute, University of California, Irvine, Irvine, CA, USA
[5]Harvard Medical School and Wellman Center for Photomedicine, Massachusetts General Hospital, Boston, MA, USA

Abstract—**A motion-sensitive *en-face*-scanning 3-D optical coherence microscope (OCM) has been designed and constructed to study critical events in the early development of plants and animals. We describe the OCM instrument and present time-lapse movies of frog gastrulation, an early developmental event in which three distinct tissue layers are established that later give rise to all major organ systems. OCM images constructed with fringe-amplitude data show the mesendoderm migrating up along the blastocoel roof, thus forming the inner two tissue layers. Motion-sigma data, measuring the random motion of scatterers, is used to construct complementary images that indicate the presence of Brownian motion in the yolk cells of the endoderm. This random motion provides additional intrinsic contrast that helps to distinguish different tissue types. Depth penetration at 850 nm is sufficient for studies of the outer ectoderm layer, but is not quite adequate for detailed study of the blastocoel floor, about 500 to 800 μm deep into the embryo. However, we measure the optical attenuation of these embryos to be about 35% less at 1310 nm. 2-D OCT images at 1310 nm are presented that promise sufficient depth penetration to test current models of cell movement near the blastocoel floor during gastrulation.**[#]

Keywords—**Developmental biology, frog gastrulation, optical coherence microscopy, optical coherence tomography**

I. Introduction

Current research in developmental biology is aimed at a full understanding of the dynamic interplay between gene expression and cell-cell signaling that results in morphogenesis of the organism. Many embryos are optically opaque, and the dynamics of developmental processes have been inferred from fixed and sectioned embryos at different time points or by observing the behavior of isolated tissue explants [1,2]. Optical coherence microscopy (OCM) offers the possibility of monitoring the dynamics of development in a single living embryo non-invasively and non-destructively.

We report here the results of OCM studies of gastrulation in the African clawed frog, *Xenopus laevis*. Cellular migrations during gastrulation establish three distinct tissue layers: an outer ectoderm, a middle mesoderm, and an inner endoderm. Directed in large part by interactions between the different layers, each layer eventually gives rise to predictable sets of tissues. The ectoderm gives rise to the skin, skull, and nervous system, including the brain and the eye. The mesoderm contributes to the heart, bones and skeletal muscle. The endoderm will develop into tissues that make up the gut and digestive organs such as the liver and pancreas [3].

Perhaps the most dramatic movement of cells during gastrulation is the involution of exterior cells to become the mesodermal cells that co-migrate with endodermal cells along the roof of the blastocoel. This process forms the inner and middle tissue layers and ultimately leads to the elongation of the embryonic axis. Recent evidence from studies of tissue explants has suggested that this process is initiated in large part by a movement of vegetal cells (endodermal cells) that has been termed "vegetal rotation" [2]. One of the goals of our OCM studies is to visualize this vegetal rotation in a single embryo *in vivo*.

The design and performance of our OCM instrument are described in Section II, and in Sections III and IV representative images of gastrulation are presented. The limited depth penetration at 850 nm causes these images to fall just short of a thorough test of the vegetal rotation model. However, a notable discovery is that Brownian motion of cell organelles can impart additional intrinsic contrast to motion-sensitive OCM images. In addition, 2-D OCT images at 1310 nm make it clear that the wavelength range 1150-1350 nm should provide sufficient depth penetration to detect unambiguously the vegetal rotation.

II. OCM instrument

The primary use of our optical coherence microscope (OCM) is to image critical events in the early development of plants and animals. Since spatial relationships between cells and groups of cells are important in the development of tissue, our OCM is designed specifically to produce 3-D images that can be rotated on a computer screen to achieve a 3-D perspective. Our current instrument provides the resolution and image acquisition speed necessary to follow *in vivo* and in real time the development of an individual frog embryo. The design principles of our OCM (Fig. 1)

[#] This work was supported by NSF grants DBI-0137973 and BES-0086924. AJS was supported by a Beckman Scholarship.

and many of the instrumental details are described in three publications [4-6]. We will summarize here the most critical performance specifications and design features.

A. Resolution

The depth resolution of our OCM is 15 μm (FWHM) in air, or 11 μm in tissue (with n = 1.4). The depth resolution is determined by the coherence length of the 850 nm superluminescent diode (SLD) used as a light source (λ_c=843nm, $\Delta\lambda_{FWHM}$=20.7nm, 1mW). The lateral resolution is 5 μm (FWHM) and corresponds to the waist diameter of the focused beam. A typical cell size in developing frog embryos is 10 μm or greater, so individual cells can sometimes be resolved. A pair of galvoscanning mirrors performs an *en face* scan of the tissue. The beam waist is moved quickly over the x-y plane, then the focusing lens is stepped down along the z-axis (depth) and a slightly deeper x-y plane is scanned. At the same time the focusing lens is moved, the reference mirror is also translated to keep the equal path length position of the OCM interferometer coincident with the focused beam waist. This procedure of "focus-tracking" maintains the 5 μm lateral resolution throughout the depth of the sample.

B. Fringes

Our OCM uses a novel, inexpensive method to produce rapidly oscillating fringes at the interferometer output. A tiny mirror (1.5 mm x 1.5 mm x 0.1 mm) is glued to a small piezoelectric stack that is in turn glued onto an aluminum disk (5 mm thick, 25.4 mm diameter) positioned at the rear of a cat's-eye retroreflector in the reference arm of the interferometer (Fig. 1). The reference beam is focused onto the mirror by the retroreflector lens, and the piezo stack is driven sinusoidally at 56.85 kHz, the resonance frequency of the drumhead mode of the aluminum disk. The amplitude of the piezo-driving voltage is set to produce a peak-to-peak displacement of 0.600 λ and hence a phase modulation of 1.2 fringes. The small amplitude of the modulation preserves the depth resolution.

The interference fringes at the output of the OCM are digitally sampled, and a partial discrete Fourier transform is performed. Because the piezo stack is driven sinusoidally, the fringe signal contains significant power in higher harmonics of the fundamental frequency ω_{mod}. We calculate the square root of the sum of the powers in $2\omega_{mod}$ and $3\omega_{mod}$ as a measure of the fringe amplitude and hence as a measure of the square root of the power backscattered from the sample. The use of these particular harmonics eliminates the effects of piezo "wobble" which are found almost exclusively in the fundamental frequency [6]. In addition, the modulation amplitude of 1.2 fringes renders this measure of the fringe amplitude insensitive to slow, thermal phase drifts in the interferometer [4].

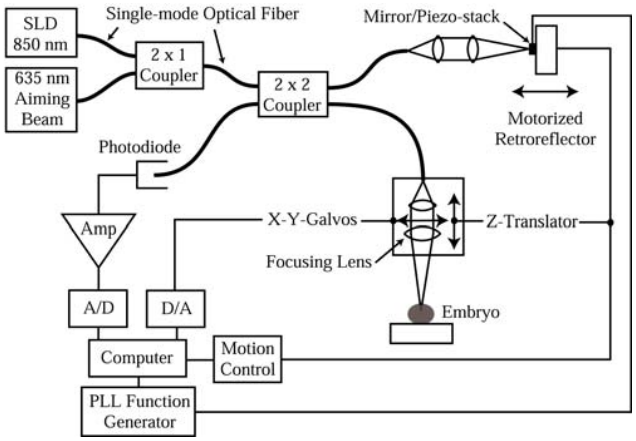

Fig. 1. Optical schematic of the OCM instrument.

C. Motion Sensitivity

The interference term (the fringe signal) of the output of our OCM is given by:

$$V(t) \propto 2\sqrt{P_{ref}P_{samp}}\cos\left[\frac{2\pi}{\lambda}[2d_{mirr}(t)+2z_{scatt}(t)]+\phi(t)\right] \qquad (1)$$

where $d_{mirr}(t)$ is the position of the oscillating reference mirror, $z_{scatt}(t)$ is the depth position (along the beam) of a scatterer, and $\phi(t)$ is a slow phase wander of the interferometer with a time scale of seconds or minutes. We drive the piezoelectric stack so that the position of the mirror obeys $d_{mirror}(t) = d_o\sin(\omega_{mod}t)$ where the modulation frequency is 56.85 kHz. The phase changes in (1) due to scatterer motion are usually slow compared to the piezo-driven phase modulation, and fast compared to the slow phase drift of the interferometer. Because of the different time scales, we can neglect the slow phase drift $\phi(t)$ in the following discussion, though its presence determines the smallest scatterer velocity that can be detected.

The phase of the fringe signal can be calculated from the discrete Fourier transform of the digitally sampled fringe signal:

$$Fringe\ Phase = \frac{4\pi}{\lambda}z_{scatt}(t) = \arctan\left(-\frac{b_3(t)}{a_2(t)}\right) \qquad (2)$$

where the Fourier coefficients b_3 and a_2 are defined by

$$Fringe\ Signal = V(t) = {a_0}/{2} + b_1\sin(\omega_{mod}t) + a_2\cos(2\omega_{mod}t) + b_3\sin(3\omega_{mod}t) + \ldots.. \qquad (3)$$

The change in phase of the fringe signal over rapid successive x-scans yields the change in depth position or the velocity of a scatterer (along the beam) [7]. If the phase

changes significantly but randomly over successive scans, the scatterer has zero mean velocity but is exhibiting random fluctuations in position and velocity (Brownian motion or diffusion) [8]. We typically perform 6 rapid successive x-scans and calculate the mean and standard deviation of the 5 phase changes. Masking out voxels with poor signal-to-noise fringe signals, we construct the so-called "motion-average" and "motion-sigma" images with the mean and standard deviation of the phase change, respectively.

D. Sensitivity

The performance of our OCM is limited by fundamental photon noise. The noise of our SLD output (~ 1 mW) is dominated by Bose-Einstein photon bunching, so we attenuate the reference beam by a factor of four to optimize the signal-to-noise ratio [4].

E. Visualization

We have written programs in the software environment of Visualization Express 6.0 (Advanced Visualization Systems, Waltham, MA) that allow us to "volume-render" our 3-D data sets onto a 2-D viewing screen (computer monitor). In this process, the contents of volume elements (voxels) are "blended" with the contents of voxels directly behind them to yield the final value assigned to a pixel on the viewing screen. An "opacity" parameter in this blending algorithm may be reduced to achieve a translucent appearance in which structures deep within the sample can be seen, or it can be increased to yield a superficial rendering of the sample. We find that rotating a translucent, volume-rendered 3-D data set is remarkably effective in producing a 3-D perspective. We can also rotate, slice, or crop the 3-D data set, yielding 2-D images that can be analyzed using standard methods. Often a 3-D perspective is used to determine the optimal 2-D slice to use in quantitative analyses. Hoeling et al. [4] describe in more detail the operation of our visualization programs.

III. OCM FRINGE-AMPLITUDE IMAGES OF GASTRULATION

Our OCM studies focused on the development of live frogs (albino *Xenopus laevis*) during gastrulation (stages 10 to 13, 10 to 15 hours post fertilization). Frog embryos of approximately 1.2 mm in diameter were held in grooves formed in 5% agarose gels. The embryos were allowed to develop at room temperature (20-23°C). Consecutive 3-D images were acquired every 10 to 15 minutes for the time period 7 to 24 hours post-fertilization. Attenuation at 850 nm is very high in these early stages of development, roughly 19/mm. Nevertheless, we were able to produce time-lapse movies from individual frog embryos of the involuting mesendodermal cells as they move up along the blastocoel roof (ectodermal layer) during gastrulation. To

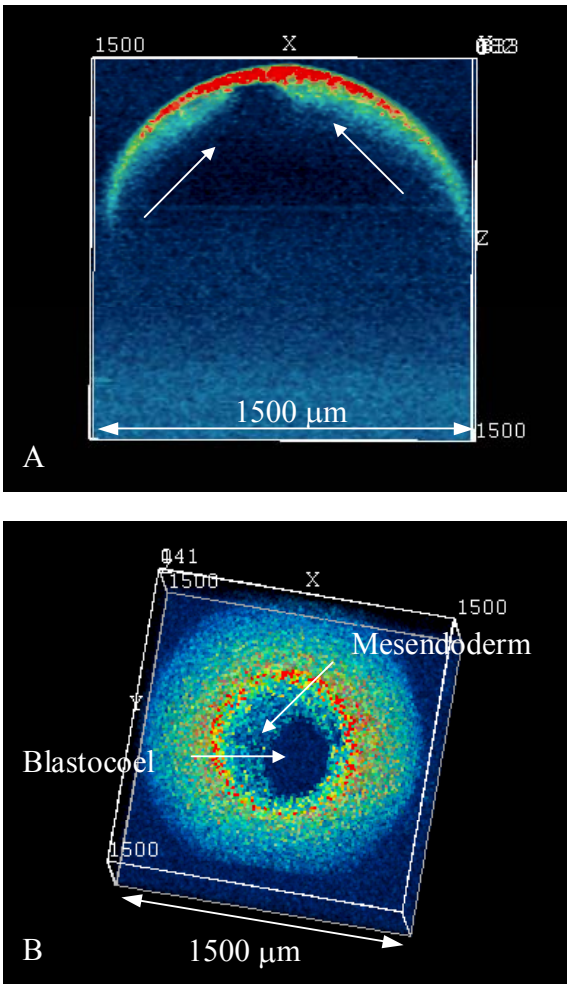

Fig. 2. Volume-rendered side-view (A) and top-view (B) of a frog embryo near the end of gastrulation. Arrows in (A) indicate the direction of motion of the mesendoderm. Red is high scattering; blue is low scattering.

the best of our knowledge, these are the first OCM movies to follow gastrulation in an individual embryo at this resolution and time scale. Fig. 2 contains two views near the end of gastrulation obtained from a single 3-D image. These views appear as corresponding frames in two time-lapse movies of gastrulation that are available on our website (http://www.physics.hmc.edu/research/ocm/). The view in Fig. 2A is a sagittal (vertical) section showing the mesendoderm moving from the periphery of the view toward a convergence spot near the top (animal pole) of the embryo. Fig. 2B is a top view looking down on the embryo. The top of the data set has been cropped off revealing the dark (low scattering) blastocoel fluid. Also visible at the periphery of the blastocoel fluid is a portion of the mesendoderm converging on a spot near the top (animal pole) of the embryo. The sense of motion provided by the time-lapse movie is essential for a full appreciation of these 3-D images.

IV. Motion-Sigma Images of Gastrulation

The blastocoel floor is noticeably absent in Fig. 2A, but is readily apparent in Fig. 3A which is constructed with motion-sigma data. Optical attenuation at 850 nm is 19/mm, so the yolk cells forming the blastocoel floor are just barely visible in fringe-amplitude images. However, motion-sigma images indicate that the yolk cells contain scatterers executing Brownian motion. We suspect the scatterers are the yolk platelets, organelles roughly 3 to 5 μm in diameter.

Two-dimensional images acquired with a 1310 nm optical Doppler tomography (OCT) instrument at the Beckman Laser Institute [7,8] show dramatically better performance. Optical attenuation at 1310 nm is reduced to 14/mm. Not only is depth penetration significantly better, but also motion-sigma images better capture the random motion present in the yolk cells. Fig. 3B is a 2-D image of two side-by-side embryos undergoing gastrulation with about a half-hour time difference in development.

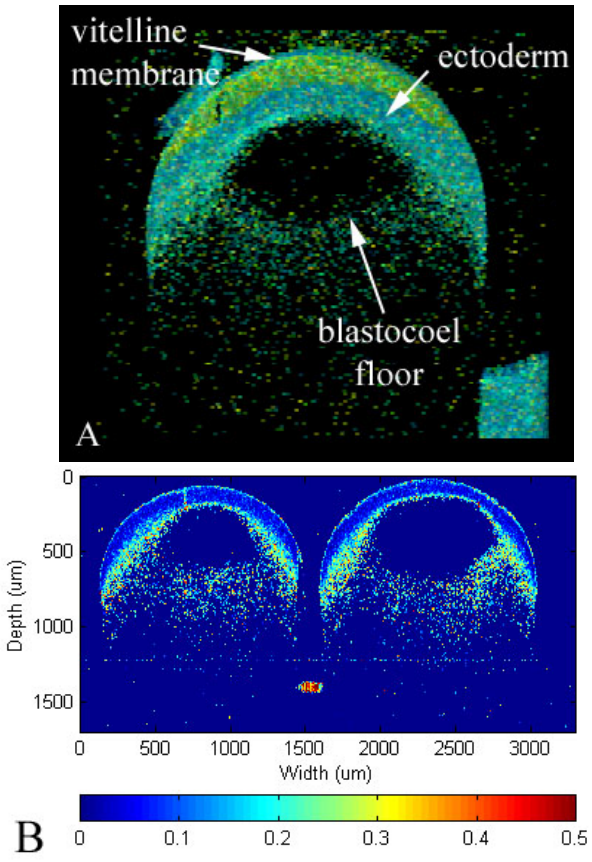

Fig. 3. Motion-sigma images of frog gastrulation. Blue is low sigma, red is high. (A) A slice through a 3-D image at 850 nm reveals the blastocoel floor. Yolk cells have a higher sigma than does the ectoderm. (B) A 2-D image at 1310 nm of two side-by-side embryos. Random motion present in the yolk cells is clearly stronger than in the ectoderm.

V. Conclusion

OCM images acquired at 850 nm capture the major cell movements involved in frog gastrulation. The ectoderm is well-visualized, as is the process of epiboly in which the ectoderm forms, thins and spreads over the exterior surface of the entire embryo. Strong attenuation at 850 nm makes it difficult to distinguish the blastocoel floor, i.e., the interface between the blastocoel fluid and the endodermal yolk cells. Motion-sigma images contain significantly more intrinsic contrast, and help to define the blastocoel floor. Vegetal rotation, observed in sectioned embryos, is not sufficiently well-visualized to confirm its existence in intact embryos.

Depth penetration is significantly improved at 1310 nm. Our 2-D OCT images at 1310 nm confirm our observations at 850 nm, and lead us to think that our recently constructed motion-sensitive 3-D OCM operating at 1310 nm will be able to answer substantive questions about frog gastrulation.

Acknowledgment

We thank Alejandro Enriquez for making gels to hold the frog embryos, and Scott Kibler for help with image acquisition.

References

[1] R. E. Keller, "Vital dye mapping of the gastrula and neurula of *Xenopus laevis* I. Prospective areas and morphogenetic movements of the superficial layer.", *Develop. Biol.* 42:222-241 (1975).

[2] R. Winklbauer, and M. Schurfeld, "Vegetal rotation, a new gastrulation movement involved in the internalization of the mesoderm and endoderm in *Xenopus*," *Development* 126:3703-3713 (1999).

[3] S. Gilbert, 2000. *Developmental Biology*. Sinauer Associates, Inc., MA.

[4] B. M. Hoeling, A. D. Fernandez, R. C. Haskell, E. Huang, W. R. Meyers, D. C. Petersen, S. E. Ungersma, R. Wang, and M. E. Williams, "An optical coherence microscope for 3-dimensional imaging in developmental biology," *Optics Express* 6: 136-146 (March 27, 2000), (http://www.opticsexpress.org/oearchive/source/19250.htm).

[5] B. M. Hoeling, A. D. Fernandez, R. C. Haskell, and D. C. Petersen, "Phase modulation at 125 kHz in a Michelson interferometer using an inexpensive piezoelectric stack driven at resonance," *Review of Scientific Instruments* 72: 1630-1633 (2001).

[6] B. M. Hoeling, M. E. Peter, D. C. Petersen, and R. C. Haskell, "Improved phase modulation for an *en-face* scanning 3D optical coherence microscope," unpublished.

[7] Y. Z. Zhao, Z. Chen, C. Saxer, S. Xiang, J. F. de Boer, and J. S. Nelson, "Phase-resolved optical coherence tomography and optical Doppler tomography for imaging blood flow in human skin with fast scanning speed and high velocity sensitivity," *Optics Letters* 25: 114-116 (2000).

[8] H. Ren, K. M. Brecke, Z. Ding, Y. Zhao, J. S. Nelson, and Z. Chen, "Imaging and quantifying transverse flow velocity with the Doppler bandwidth in a phase-resolved functional optical coherence tomography," *Opt. Lett.* 27: 409-411 (2002).